Spectrum Efficient Single-Sideband Single-Carrier with Frequency-Domain Equalization

Kohei ABO† Thanh Hai VO† Amnart BOONKAJAY† and Fumiyuki ADACHI‡
Dept. of Communications Engineering, Graduate School of Engineering, Tohoku University
6-6-05 Aza-Aoba, Aramaki, Aoba-ku, Sendai, 980-8579 Japan
†{abo, vothanhhai, amnart}@mobile.ecei.tohoku.ac.jp, ‡adachi@ecei.tohoku.ac.jp

***Abstract*—In this paper, a novel spectrum efficient single-sideband single-carrier (SC) with frequency-domain equalization (SSB-FDE) using amplitude shift keying (ASK) modulation (ASK SSB-FDE) is proposed. Similar to the conventional SC transmission with FDE (SC-FDE), the ASK modulated symbol block to be transmitted is transformed by discrete Fourier transform (DFT) into frequency-domain signal. Then, inverse DFT (IDFT) is applied to the upper (or lower) sideband spectrum to obtain the time-domain SSB signal block. The cyclic prefix (CP) inserted SSB signal block is transmitted over a frequency-selective fading channel. At a receiver, the minimum mean square error (MMSE) based FDE is applied. ASK SSB-FDE has lower peak-to-average power ratio (PAPR) and better throughput performance than QAM SC-FDE when the throughput is plotted as a function of peak transmit SNR. This is confirmed by computer simulation assuming a frequency-selective Rayleigh fading channel.**

Keywords—single-sideband; amplitude shift keying; frequency-domain equalization

I. INTRODUCTION

The frequency-domain equalization based on minimum mean square error criterion (MMSE-FDE) can take advantage of the channel frequency-selectivity to improve the bit error rate (BER) performance of the broadband single-carrier (SC) transmission [1-3]. SC-FDE is one of promising broadband signal transmission techniques. Recently, improving the spectrum efficiency (SE) in broadband transmission is becoming a serious problem because of a rapid growth of wireless data traffic while the available bandwidth is limited. Many works aiming to increase SE also have been recently published such as faster-than-Nyquist (FTN) transmit filtering [4] and partial response (PR) transmit filtering [5]. Even though those transmission techniques in [4, 5] can achieve higher SE, the error probability becomes worse since those transmission increase interference.

Analog single-sideband (SSB) transmission technique [6] utilizes a complex conjugate relationship between the upper sideband (USB) and lower sideband (LSB) to transmit either USB or LSB components. SSB can therefore double the SE compared to SC-FDE (which is double sideband transmission). Recently, we proposed analog SSB-FDE [7], which can halve the signal bandwidth while keeping the transmission quality the same as analog SC-FDE. Can SSB technique be applied to SC-FDE using spectrum efficient quadrature amplitude modulation (QAM)? This is an interesting question. Unfortunately, SSB technique cannot directly be applied to QAM SC-FDE since the low-pass equivalent signal of QAM SC signal is a complex-valued signal and hence, it does not have a complex conjugate relationship between the USB and LSB components. On the other hand, the low-pass equivalent signal of amplitude shift keying (ASK) SC signal is real-valued and hence, SSB can be applied to halve the transmission signal bandwidth. This observation motivates us to apply the SSB technique to ASK SC transmission.

In this paper, we propose a spectrum efficient ASK SSB-FDE. A theoretical analysis on the BER of ASK SSB-FDE is given. The superiority of ASK SSB-FDE is confirmed by computer simulation assuming a frequency-selective Rayleigh fading channel, at which the ASK SSB-FDE achieves lower peak-to-average power ratio (PAPR) and better throughput performance than QAM SC-FDE when the throughput is plotted as a function of peak transmit SNR.

The remainder of this paper is organized as follows. Sect. II describes the system model of ASK SSB-FDE and Sect. III presents the BER analysis. Computer simulation results are presented and discussed in Sect. IV. Sect. V concludes the paper.

II. ASK SSB-FDE

Transmission system model of ASK SSB-FDE and signal constellation of M-ASK modulation (M = 2, 4, 8) are illustrated in Fig. 1 and Fig. 2, respectively. Gray code mapping is assumed. In order to make a fair performance comparison using the same transmission bandwidth, the sample duration of ASK SSB-FDE is set to $T_s/2$, where T_s is the sample duration of QAM SC-FDE.

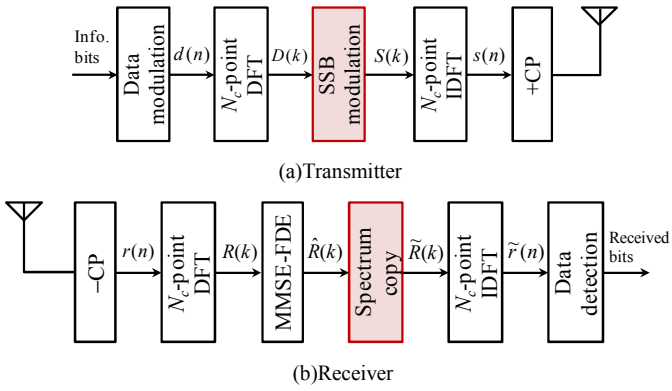

Fig. 1. Transmission system model of ASK SSB-FDE.

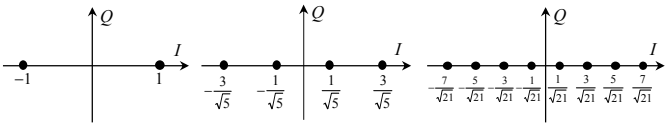

(a)2ASK (b)4ASK (c)8ASK

Fig. 2. Signal constellation of ASK modulation.

A. Transmit Signal Representation

ASK-modulated data symbol block $\{d(n);\ n=0\sim N_c-1\}$ is real-valued and hence, SSB can be applied. $d(n)$ is given by [8]

$$d(n)=(2m-1-M)\sqrt{\frac{3}{M^2-1}}\quad ,m=1,2,...,M\ . \tag{1}$$

N_c-symbol sequence $\{d(n);\ n=0\sim N_c-1\}$ is transformed into the frequency-domain signal $\{D(k);\ k=0\sim N_c-1\}$ by applying N_c-point discrete Fourier transform (DFT). $D(k)$ is given by

$$D(k)=\sqrt{1/N_c}\sum_{n=0}^{N_c-1}d(n)\exp\left(-j2\pi kn/N_c\right). \tag{2}$$

Since $\{d(n);\ n=0\sim N_c-1\}$ is a real-valued sequence, the frequency-domain signal $\{D(N_c-k);\ k=1\sim N_c/2-1\}$ can be expressed as

$$\begin{aligned}D(N_c-k)&=\sqrt{1/N_c}\sum_{n=0}^{N_c-1}d(n)\exp\left(-j2\pi(N_c-k)n/N_c\right)\\&=\left[\sqrt{1/N_c}\sum_{n=0}^{N_c-1}d(n)\exp\left(-j2\pi kn/N_c\right)\right]^*\\&=D^*(k)\end{aligned}\quad . \tag{3}$$

It can be seen from Eq. (3) that the frequency-domain signal $\{D(k);\ k=0\sim N_c-1\}$ can be reproduced from either $\{D(k);\ k=0\sim N_c/2\}$ or $\{D(k);\ k=0,\ N_c/2\sim N_c-1\}$. SSB spectrum $\{S(k);\ k=0\sim N_c/2\}$ is obtained by applying low-pass filter (LPF) for removing $\{D(k);\ k=N_c/2+1\sim N_c-1\}$. $S(k)$ is given by

$$S(k)=\begin{cases}D(k) & ,k=0\sim N_c/2\\ 0 & ,k=N_c/2+1\sim N_c-1\end{cases}, \tag{4}$$

Then, N_c-point inverse DFT (IDFT) is applied to transform the frequency-domain signal $\{S(k);\ k=0\sim N_c-1\}$ into time-domain signal $\{s(n);\ n=0\sim N_c-1\}$, which is expressed as

$$s(n)=\sqrt{4E_s/T_s}\sqrt{1/N_c}\,\varepsilon\cdot\sum_{k=0}^{N_c-1}S(k)\exp\left(j2\pi nk/N_c\right), \tag{5}$$

where E_s is the symbol energy, $T_s/2$ is the sample duration and where $\varepsilon=\sqrt{2N_c/(N_c+2)}$ is the power-normalization factor.

To avoid the inter-block interference (IBI), the last N_g samples of each transmission block are copied as a cyclic prefix (CP) and inserted into the guard interval (GI) placed at the beginning of each bock.

B. Received Signal Representation

We assume a frequency-selective block Rayleigh fading channel having L distinct propagation paths. The channel impulse response $\{h(\tau);\ \tau=0\sim L-1\}$ is given by

$$h(\tau)=\sum_{l=0}^{L-1}h_l\cdot\delta(2\tau-\tau_l), \tag{6}$$

where τ_l is the delay time and h_l is the complex-valued path gain with $E[\sum_{l=0}^{L-1}|h_l|^2\ ]=1$and assuming $\tau_l=2l$.

The CP-removed received signal $\{r(n);\ n=0\sim N_c-1\}$ can be expressed as

$$r(n)=\sum_{l=0}^{L-1}h_l\cdot s\left((n-\tau_l)\bmod N_c\right)+\eta(n), \tag{7}$$

where $\eta(n)$ denotes the zero-mean complex-valued Gaussian noise having variance $4N_0/T_s$ with N_0 being the one-sided power spectrum density of additive white Gaussian noise (AWGN). N_c-point DFT is then applied to obtain frequency-domain received signal $\{R(k);\ k=0\sim N_c-1\}$ as

$$R(k)=\sqrt{4E_s/T_s}\,\varepsilon\cdot S(k)H(k)+\Pi(k), \tag{8}$$

where $H(k)$ and $\Pi(k)$, $k=0\sim N_c-1$, are respectively the frequency-domain channel gain and the noise component which are given by

$$\begin{cases}H(k)=\sum_{l=0}^{L-1}h_l\exp\left(-j2\pi k\tau_l/N_c\right)\\ \Pi(k)=\sqrt{1/N_c}\sum_{n=0}^{N_c-1}\eta(n)\exp\left(-j2\pi kn/N_c\right)\end{cases}. \tag{9}$$

Then, MMSE-FDE is performed to take advantage of the channel frequency-selectivity as

$$\begin{aligned}\hat{R}(k)&=R(k)W(k)\\&=\sqrt{4E_s/T_s}\,\varepsilon\cdot D(k)H(k)W(k)+\Pi(k)W(k)\quad ,k=0\sim N_c/2\end{aligned}, \tag{10}$$

where $W(k)$, $k=0\sim N_c/2$, is one-tap MMSE-FDE weight which is designed to minimize the mean square error (MSE) between $\hat{R}(k)$ and $D(k)$. $W(k)$ is given as [9]

$$W(k)=\frac{H^*(k)}{|H(k)|^2+(\varepsilon^2\cdot E_s/N_0)^{-1}}. \tag{11}$$

Next, SSB demodulation is performed to obtain $\{\widetilde{R}(k);\ k=0\sim N_c-1\}$ as [7]

$$\begin{aligned}\widetilde{R}(k)&=\begin{cases}\hat{R}(k) & ,k=0\sim N_c/2\\ \hat{R}^*(N_c-k) & ,otherwise\end{cases}\\&=\sqrt{4E_s/T_s}\,\varepsilon\cdot D(k)\widetilde{H}(k)\widetilde{W}(k)+\widetilde{\Pi}(k)\widetilde{W}(k)\end{aligned}\quad , \tag{12}$$

where

$$\begin{cases}\widetilde{H}(k)=H(k),\ \widetilde{W}(k)=W(k), \\ \widetilde{\Pi}(k)=\Pi(k)\end{cases} ,k=0\sim\frac{N_c}{2}$$
$$\begin{cases}\widetilde{H}(k)=H^*(N_c-k),\ \widetilde{W}(k)=W^*(N_c-k), \\ \widetilde{\Pi}(k)=\Pi^*(N_c-k)\end{cases} ,k=\frac{N_c}{2}+1\sim N_c-1 \quad (13)$$

Note that Eq. (12) can be written based on the complex conjugate relationship in Eq. (3).

After SSB demodulation, N_c-point IDFT is applied to transform the frequency-domain signal $\{\widetilde{R}(k);\ k=0\sim N_c-1\}$ into the time-domain signal $\{\widetilde{r}(n);n=0\sim N_c-1\}$ for data demodulation as

$$\widetilde{r}(n)=\sqrt{1/N_c}\sum_{k=0}^{N_c-1}\widetilde{R}(k)\exp\left(j2\pi nk/N_c\right). \quad (14)$$

III. BER ANALYSIS

The time-domain signal $\{\widetilde{r}(n);n=0\sim N_c-1\}$ after SSB demodulation in ASK SSB-FDE can be expressed as [10]

$$\widetilde{r}(n)=\sqrt{4E_s/T_s}\,\varepsilon\cdot A\cdot d(n)+\mu_{SSB}(n), \quad (15)$$

where

$$\begin{cases}A=\left(1/N_c\right)\sum_{k=0}^{N_c-1}\widetilde{H}(k)\widetilde{W}(k)=\left(1/N_c\right)\sum_{k=0}^{N_c-1}\frac{|\widetilde{H}(k)|^2}{|\widetilde{H}(k)|^2+(\varepsilon^2\cdot E_s/N_0)^{-1}} \\ \mu_{SSB}(n)=\mu_{ISI}(n)+\widetilde{\eta}(n)\end{cases} \quad (16)$$

with

$$\begin{cases}\mu_{ISI}(n)=\sqrt{4E_s/T_s}\left(\varepsilon/\sqrt{N_c}\right)\sum_{k=0}^{N_c-1}\left[\begin{matrix}\left\{\widetilde{H}(k)\widetilde{W}(k)-A\right\} \\ \cdot D(k)\exp\left(j2\pi nk/N_c\right)\end{matrix}\right] \\ \widetilde{\eta}(n)=\sqrt{1/N_c}\sum_{k=0}^{N_c-1}\widetilde{\Pi}(k)\widetilde{W}(k)\exp\left(j2\pi nk/N_c\right)\end{cases}. \quad (17)$$

It can be understood from Eqs. (15) and (16) that $\widetilde{r}(n)$ is real-valued random variable with mean $\sqrt{4E_s/T_s}\,\varepsilon\cdot A\cdot d(n)$. $\mu_{ISI}(n)$ and $\widetilde{\eta}(n)$ are the residual ISI and the noise after performing MMSE-FDE, respectively. The (N_c-k)-th frequency component $M_{SSB}(N_c-k)$ of $\mu_{SSB}(n)$ can be expressed as

$$\begin{aligned}&M_{SSB}(N_c-k)\\&=\sqrt{1/N_c}\sum_{n=0}^{N_c-1}\mu_{SSB}(n)\exp\left(-j2\pi(N_c-k)n/N_c\right)\\&=\left[\sqrt{4E_s/T_s}\,\varepsilon\left\{\widetilde{H}(k)\widetilde{W}(k)-A\right\}D(k)+\widetilde{\Pi}(k)\widetilde{W}(k)\right]^*\\&=M_{SSB}^*(k)\end{aligned}, \quad (18)$$

where conjugate relation shown in Eq. (13) is used. Eq. (18) shows that $\mu_{SSB}(n)$ is real-valued. Assuming that $\mu_{ISI}(n)$ is a zero-mean real-valued Gaussian variable, $\mu_{SSB}(n)$ can be treated as a new zero-mean real-valued Gaussian variable. The variance of $\mathrm{Re}[\mu_{SSB}(n)]$ is given by [10]

$$\sigma_{SSB}^2\approx\frac{4N_0}{T_s}\left[\begin{matrix}\left(2E_s/N_0\right)\left\{\left(1/N_c\right)\sum_{k=0}^{N_c-1}|\widetilde{H}(k)\widetilde{W}(k)|^2-A^2\right\}\\+\left(1/N_c\right)\sum_{k=0}^{N_c-1}|\widetilde{W}(k)|^2\end{matrix}\right]. \quad (19)$$

Note that $\varepsilon(=\sqrt{2N_c/(N_c+2)})$ is approximately $\sqrt{2}$ for a sufficiently large value of N_c. The conditional BER of 2ASK SSB-FDE for the given E_b/N_0 and $\{\widetilde{H}(k);\ k=0\sim N_c-1\}$ can be obtained as [8]

$$\begin{aligned}&p_{\substack{\mathrm{2ASK}\\\mathrm{SSB}}}\left(\frac{E_b}{N_0}\right)\\&=\mathrm{Prob}\left[\mathrm{Re}[\widetilde{r}(n)]<0\,|\,\{\widetilde{H}(k)\}\right]\\&=\int_{-\infty}^{0}\frac{1}{\sqrt{2\pi}\,\sigma_{SSB}}\exp\left(-\frac{\left|\mathrm{Re}[\widetilde{r}(n)]-\sqrt{4E_s/T_s}\,\varepsilon\cdot A\right|^2}{2\sigma_{SSB}^2}\right)d\widetilde{r}(n)\\&=\frac{1}{2}erfc\left(\sqrt{\gamma\left(\frac{E_b}{N_0}\right)}\right)\end{aligned}, \quad (20)$$

where

$$\gamma\left(\frac{E_b}{N_0}\right)=\frac{\frac{N_c}{N_c+N_g}\left(\frac{E_b}{N_0}\right)\cdot A^2}{\left[\begin{matrix}\frac{2N_c}{N_c+N_g}\left(\frac{E_b}{N_0}\right)\left\{\frac{1}{N_c}\sum_{k=0}^{N_c-1}|\widetilde{H}(k)\widetilde{W}(k)|^2-A^2\right\}\\+\frac{1}{N_c}\sum_{k=0}^{N_c-1}|\widetilde{W}(k)|^2\end{matrix}\right]}. \quad (21)$$

Eq. (20) is identical to the conditional BER of 4QAM SC-FDE [10]. The conditional BER of 4ASK/8ASK SSB-FDE can be derived similarly to Eq. (20). The conditional BER of 4ASK(8ASK) SSB-FDE can be shown to be the same as that of 16QAM(64QAM) SC-FDE. The above shows that MASK SSB-FDE and M^2 QAM SC-FDE provide the identical BER performance.

TABLE I. SIMULATION CONDITION

Transmitter	Data modulation	MASK SSB (M = 2, 4, 8)	MASK (M = 2, 4, 8) MQAM (M = 4, 16, 64)
	DFT size	N_c = 512	$N_c/2$ = 256
	CP length	N_g = 32	$N_g/2$ = 16
Channel	Fading type	Frequency-selective block Rayleigh	
	Power delay profile	L=16 path uniform power delay profile	
Receiver	Channel estimation	Ideal	
	Equalization	MMSE-FDE	

IV. COMPUTER SIMULATION

Simulation parameters are shown in Table I. Performance evaluation is organized in aspects of PAPR, BER, and throughput. For QAM/ASK SC-FDE, the sample duration is T_s and DFT-size is $N_c/2$ [11] in order to compare the performance using the same bandwidth as MASK SSB-FDE.

A. PAPR

The signal trajectories are shown in Fig. 3 for 2ASK SSB and 4QAM. Fig. 4 shows the cumulative distribution function (CCDF) curves of PAPR for 2ASK SSB, 2ASK, and 4QAM. PAPR is defined as

$$PAPR = \frac{\max\{|s(n)|^2; n = 0,1/V,2/V,...,N_c - 1\}}{E[|s(n)|^2]}, \quad (22)$$

where V is oversampling factor. We evaluate the complementary CCDF at $V = 8$. It is seen from Fig. 4 that the PAPR of 2ASK SSB is lower than those of 2ASK and 4QAM.

Fig. 5 shows SE-PAPR value at probability of occurrence equals 0.1% ($PAPR_{0.1\%}$) relationship of ASK SSB, ASK, and QAM. It can be seen from Fig. 5 that 2ASK/4ASK/8ASK SSB reduces $PAPR_{0.1\%}$ by about 1.2dB/0.8dB/0.6dB compared to 4QAM/16QAM/64QAM.

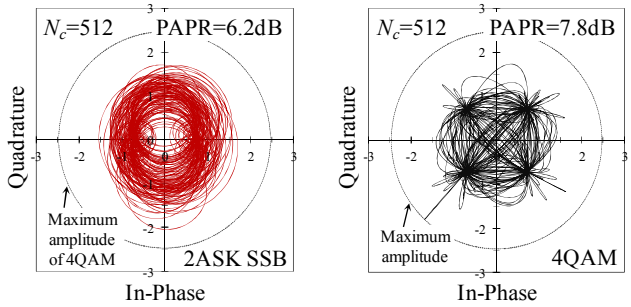

Fig. 3. Signal trajectories of 2ASK SSB and 4QAM.

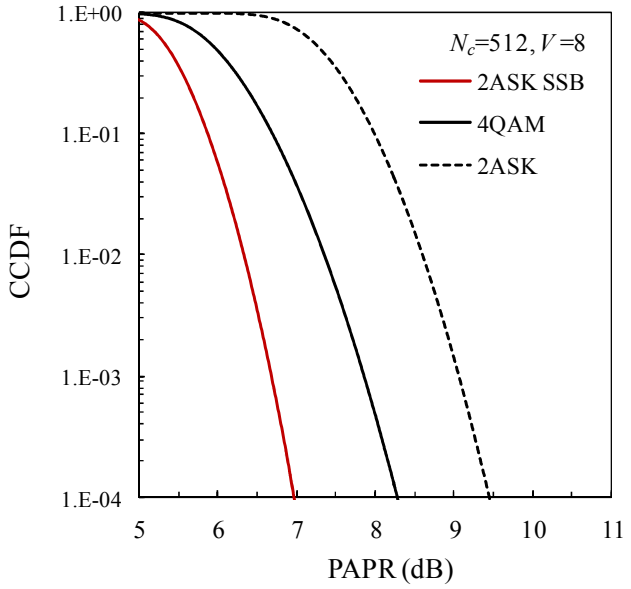

Fig. 4. PAPR comparison among 2ASK SSB, 2ASK and 4QAM.

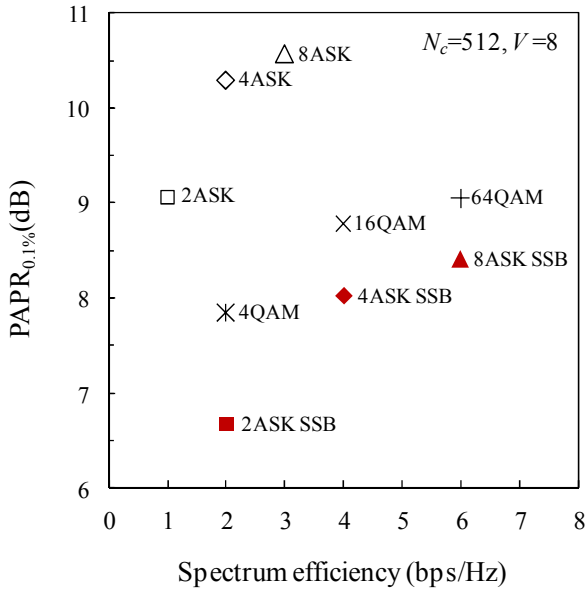

Fig. 5. SE–$PAPR_{0.1\%}$ of ASK SSB, ASK and QAM.

B. Average BER performance

The average BER performance in ideal channel estimation of MASK SSB-FDE (M = 2, 4, 8) are plotted in Fig. 6 as a function of the average received bit energy-to-noise power spectrum density ratio $E_b/N_0 = (1/\log_2 M)(E_s/N_0)(1+N_g/N_c)$. The numerical evaluation of theoretical BER is done based on Monte-Carlo method [10]. MASK SSB-FDE has the same BER performance as M^2 QAM SC-FDE. In addition, a fairly good agreement is observed between the theoretical and simulation results.

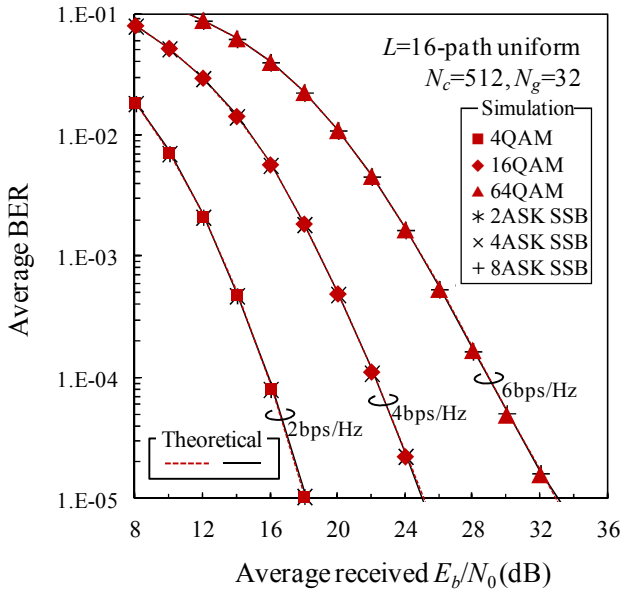

Fig. 6. Average BER performance of ASK SSB-FDE and QAM SC-FDE.

C. *Throughput performance*

Throughput η_{SSB}^{ASK} (bps/Hz) of ASK SSB-FDE and throughput η^{QAM} (bps/Hz) of QAM SC-FDE is defined by

$$\begin{cases} \eta_{SSB}^{ASK} = \varepsilon^2 \cdot \log_2 M \times (1-\mathrm{PER}) \times N_c/(N_c+N_g) \\ \eta^{QAM} = \log_2 M \times (1-\mathrm{PER}) \times N_c/(N_c+N_g) \end{cases}, \quad (23)$$

where PER represents packet error rate. A packet consists of 3072 information bits. The throughput performance under ideal channel estimation is plotted as a function of peak transmit SNR in Fig. 7, where the peak transmit SNR is defined as the average received SNR plus $\mathrm{PAPR}_{0.1\%}$ [12]. The peak transmit SNR is considered as an important design parameter of power amplifiers. The average received SNR is defined as $2E_s/N_0$ for ASK SSB and E_s/N_0 for QAM. When the throughput is plotted as a function of peak transmit SNR, ASK SSB-FDE provides better performance compared to QAM SC-FDE since ASK SSB-FDE provides the same BER performance and lower PAPR compared to QAM SC-FDE.

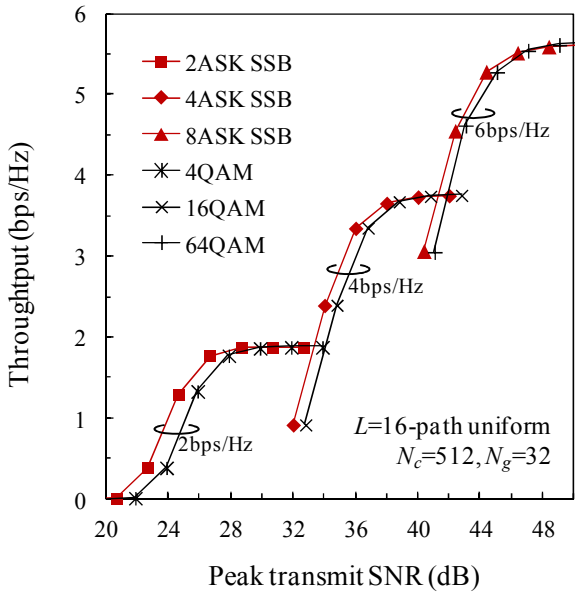

Fig. 7. Throughtput performance.

V. CONCLUSION

In this paper, we proposed a spectrum efficient ASK SSB-FDE in order to improve SE in broadband transmission. ASK SC signal has a complex conjugate relationship between the USB and LSB components and hence, SSB technique can be applied to halve the transmission signal bandwidth. It is shown by both theoretical analysis and simulation that ASK SSB-FDE achieves lower PAPR and better peak transmit SNR-throughput performance compared to QAM SC-FDE.

REFERENCES

[1] D. Falconer, S.L. Ariyavisitakul, A. Benyamin-Seeyar, and B. Edison, "Frequency domain equalization for single-carrier broadband wireless systems," IEEE Commun. Mag., vol. 40, no. 4, pp. 58-66, Apr. 2002.

[2] F. Adachi, D. Garg, S. Takaoka, and K. Takeda, "Broadband CDMA techniques," IEEE Wireless Commun. Mag., vol. 12, no. 2, pp. 8-18, Apr. 2005.

[3] H. Sari, G. Karam, and I. Jeanclaude, "Transmission techniques for digital terrestrial TV broadcasting," IEEE Commun. Mag., vol. 33, pp. 100-109, Feb. 1995.

[4] S. Sugiura, "Frequency-domain equalization of faster-than Nyquist signaling," IEEE Wireless Commun. Lett., vol. 2, no.5, pp.555-558, Oct. 2013.

[5] K. Abo, A. Boonkajay, T. Yamamoto, and F. Adachi, "Duobinary PR response filtered SC-FDE," Proc. The 10th IEEE Vehicular Technology Society Asia Pacific Wireless Communications Symposium (APWCS 2013), Seoul, Korea 22–23 Aug. 2013.

[6] Carl F. Kurth, "Generation of single-sideband signals in multiplex communication systems," IEEE Trans. on Circuits and Systems, vol. cas-23, no.1, pp.1-17, June 1976.

[7] T.H. Vo, S. Kumagai, and F. Adachi, "Analog SC-FDE using single sideband technique," Proc. The 2014 International Conference on Advanced Technologies for Communications (ATC), Hanoi, Vietnam, Oct. 2014.

[8] J.G. Proakis and M. Salehi, Digital Communications, 5th ed., McGraw-Hill, 2008.

[9] F. Adachi, H. Tomeba, and K. Takeda, "Introduction of frequency-domain signal processing to broadband single-carrier transmission in a wireless channel," IEICE Trans. Commun., vol. E92-B, no. 9, pp. 2789-2808, Sept. 2009.

[10] F. Adachi and K. Takeda, "Bit error rate analysis of DS-CDMA with joint frequency-domain equalization and antenna diversity combining," IEICE Trans. Commun., vol. E87-B, no. 10, pp. 2991-3002, Oct. 2004.

[11] F. Adachi, H. Tomeba, and Kazuki Takeda, "Frequency-domain equalization for broadband single-carrier multiple access," IEICE Trans. Commun., vol. E92-B, no.05, pp. 1441-1456, May 2009.

[12] H. Gacanin and F. Adachi, "A Comprehensive Performance Comparison of OFDM/TDM Using MMSE-FDE and Conventional OFDM," Proc. IEEE 67th Veh. Technol. Conf. (VTC), pp.11-14, May, 2008.